Design Update on the MAST-Upgrade Microwave Heating and Current Drive System Launchers

Joe O. Allen, Shail Desai, Simon Freethy, Keith Hawkins, Mark A. Henderson, Carsten Lechte, Jonathan Pearl, Burkhard Plaum, and Helen Webster, and the MAST-U EBW Team

***Abstract*— MAST-Upgrade (MAST-U) is undergoing several enhancements to deliver increased performance and functionality. One such enhancement is the design, development, and implementation of an electron Bernstein wave (EBW) heating and current drive (HCD) system. The MAST-U EBW System aims to provide experimental data for model validation, along with a greater understanding of EBW physics and its capabilities. The MAST-U EBW System will deliver up to 1.8 MW of microwave power via two microwave beams, at the dual frequencies of 28 and 34.8 GHz for up to 4.5 s. This article provides an update on the system's in-vessel components, with particular focus on the quasi-optical launcher design and modeled performance.**

***Index Terms*— Current drive, electron Bernstein wave (EBW), heating, MAST-Upgrade (MAST-U), microwaves, start-up.**

I. Introduction

SEVERAL projects are underway to enhance the capability of MAST-Upgrade (MAST-U), one being the addition of an electron Bernstein wave (EBW) microwave heating and current drive (HCD) system at 28 and 34.8 GHz. Two gyrotrons will produce a total of 1.8 MW of microwave power, with ∼1.5 to 1.6 MW delivered to the plasma, due to transmission line and launcher losses. The two microwave beams are injected from the low-field side and coupled into the plasma via the two-stage O-X-B mode conversion process [1], [2], [3]. Modeling suggests current drive efficiencies between 0.1 and 0.14 A/W (normalized efficiency $\zeta = 0.43$–0.6), meaning the microwave power into the plasma will drive between 130 and 200 kA, assuming 90% coupling efficiency [4]. The MAST-U EBW project aims to provide experimental data relevant for the STEP HCD system and other spherical tokamaks. See [4] for the physics and modeling driving the design and [5], [6] for engineering overviews of the system.

II. Quasi-Optical Launchers

Meeting project requirements necessitates a variety of launch options: on- and off-axis current drive, co- and counter-current drive, and balanced co- and counter-current injection for pure heating. Waveguide switches are used to direct the beam from each gyrotron to either the upper or midplane launcher. In order to optimize the microwave-plasma coupling, the beams should be steerable in the toroidal and poloidal directions around the optimum injection vector. In addition, the system should provide microwave assisted start-up capability. Balanced co- and counter-current injection (zero net current) is most straightforward to achieve by launching beams from the midplane of MAST-U, one directed upward to drive current parallel to the plasma current and the other directed below the midplane (in opposite toroidal directions) to drive current antiparallel to the plasma current. Differences in gyrotron power and coupling efficiency of each launcher will need to be accounted for the net current driven to be close to zero.

Additional midplane launcher steering covers a range of plasma scenarios in both the co- and counter-current directions. Microwave-plasma coupling through the O-X-B conversion process is strongly influenced by the divergence on the O-mode beam injected into the plasma. In general, the larger the Gaussian beam waist (the narrowest the radius the beam is focused to), the lower the divergence of the beam, resulting in greater coupling efficiency [4]. An in-vessel view of the midplane and upper EBW launchers (on- and off-axes) is shown in Fig. 1, with mirrors depicted in blue and green and including the beam envelopes and steering ranges into the plasma.

A. On-Axis/Midplane Launcher

To deliver pure heating (balanced current drive), we have designed two midplane quasi-optical launch paths, which can inject the microwave beams symmetrically either above or below the MAST-U midplane. These launchers are named delta (D) and epsilon (E), corresponding to the system's two gyrotrons, and consist of a focusing mirror (M1) and a steering mirror (M2). Sketches of the beam propagation through the delta (blue) and epsilon (insert, green) optics are drawn in Fig. 2, showing the expansion of the microwave beams, as they propagate from the waveguide aperture through the mirror arrangement.

All focusing mirrors in the quasi-optical systems presented here are created from ellipsoids of revolution (an ellipse revolved around its major axis), giving the mirror an input and output focal point to focus a beam through the optical path. The one slight exception is DM1, which has a virtual output focal point behind the mirror surface. This enables the midplane delta launcher to inject power both in flat-top plasma operation and during start-up. The main constraints

Manuscript received 3 October 2023; revised 14 March 2024; accepted 4 June 2024. Date of publication 4 September 2024; date of current version 9 December 2024. This work was supported in part by Engineering and Physical Sciences Research Council (EPSRC) Energy Program under Grant EP/W006839/1. The review of this article was arranged by Senior Editor R. Chapman. *(Corresponding author: Joe O. Allen.)*

Joe O. Allen, Shail Desai, Simon Freethy, Keith Hawkins, Mark A. Henderson, Jonathan Pearl, and Helen Webster are with UKAEA, Culham Science Center, OX14 3DB Abingdon, U.K. (e-mail: joe.allen@ukaea.uk).

Carsten Lechte and Burkhard Plaum are with IGVP, University of Stuttgart, 70569 Stuttgart, Germany.

Color versions of one or more figures in this article are available at https://doi.org/10.1109/TPS.2024.3410644.

Digital Object Identifier 10.1109/TPS.2024.3410644

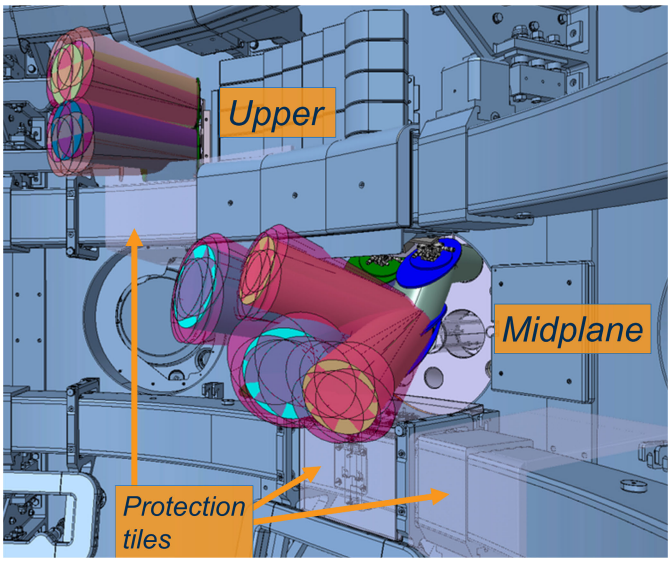

Fig. 1. Midplane and upper launcher models showing injected beam paths for a range of plasma scenarios and steering angles. Solid cones indicate the nominal injected direction, which are surrounded by translucent cones describing the extremities of a given mirror's steering range. Midplane mirrors are visible in green (delta) and blue (epsilon), and an example mounting bracket is included. Only the upper steering mirrors can be seen, as the rest are either hidden by the beam cones or not visible. Orange arrows direct the reader to faintly visible L-shaped graphite protection plates for scattering uncoupled microwave power, discussed in Section IV.

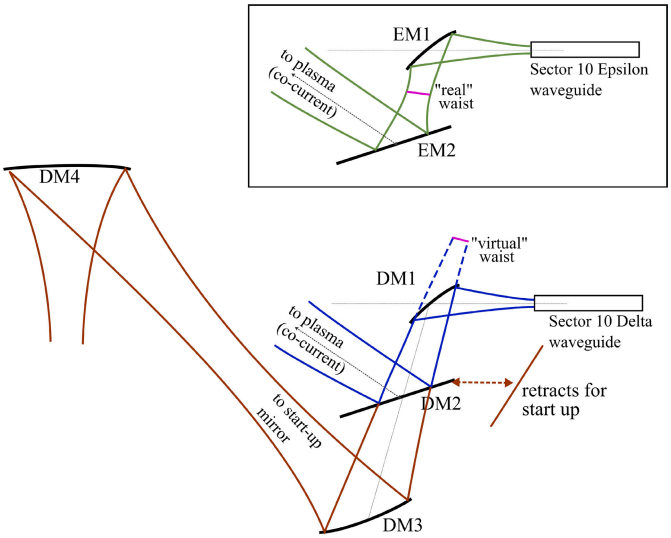

Fig. 2. Sketch of the on-axis launcher paths for the two gyrotron beams, delta and epsilon, showing the difference in focusing of the M1s and the alternate start-up operational mode for the delta launcher (red). The mirrors and beams are effectively flattened onto a poloidal plane. The insert shows the epsilon beam profile (green), where EM1 is part of an ellipsoid of revolution surface to focus the beam onto the EM2 steering mirror. We designed DM1 as a modified ellipsoid of revolution, to give a "virtual" output beam waist behind its reflective surface, which matches the required delta beam (blue) radii at DM2 and DM3.

driving the design of the midplane launcher are as follows: the midplane port through which the beams are transmitted is currently an entry port for in-vessel access; therefore, the launcher assembly must be contained within the DN600 port area so as to be easily removable during machine shutdown for maintenance, restricting the mirror locations and dimensions. MAST-U's machine parameters dictate the chosen gyrotron frequencies, 28 and 34.8 GHz, which are lower than typical for microwave heating systems, and so, the optics here must accommodate the relatively greater beam divergence. As explained above, the steering mirrors must be on the midplane to provide balanced, zero net-current injection, which restricts their locations further. In addition, a wide angular steering range is required to cover these two main injection directions, so the M1s should ideally be positioned on a vector perpendicular to these two directions (the primary M2 rotation axis) in order to minimize the M2 dimensions. The steering mirrors should be flat to prevent potential astigmatism introduced by misalignment when steering a curved mirror, meaning that the launcher focusing and coupling efficiency are dictated by the distance from the waveguide apertures to the corresponding M1s. An output beam waist of at least 6λ is targeted to achieve $\sim$90% or greater coupling efficiency. Coupled with the requirement for each mirror to capture $\geq$99% of the incident beam at 28 GHz, this drives the mirror dimensions to increase. The two waveguides enter the vacuum vessel port parallel and in a horizontal plane, so the M1s and M2s sit side by side, as can be seen in Fig. 1. In this CAD image, the solid cones represent the 99% power beam diameter through the two mirrors and into the nominal co- and counter-current plasma coupling windows. The translucent pink cones show the extents of the steering range in each main direction for optimal coupling to plasmas with a range of parameters and including $\pm 5^\circ$ steering in the toroidal and poloidal axes. An equivalent set of output beam cones can be seen for the upper launcher, which will be described in the following section.

B. Start-Up Launcher

One midplane launcher (delta) has a dual function to deliver high-field side injection during plasma start-up, following up on microwave-assisted start-up experiments on MAST [7] with tenfold increases in power and beam pulse duration. A polarizer grating tile is already installed on the center column (CC) to reflect the injected O-mode into X-mode, which is absorbed at the plasma resonance above the midplane, driving current parallel to that driven by the solenoid.

To provide this capability while retaining as much efficiency and access during flat-top operation, we include the DM3 mirror underneath DM2, along the DM1–DM2 vector. The semitransparent blue cones in Fig. 3 show the beam path of this alternative configuration of the midplane delta launcher up to the CC polarizer. The steering mirror DM2 is retractable toward the vessel port allowing the beam to pass to M3, which focuses the beam over 2.3 m onto M4, located in the machine sector containing the CC tile. The beam converges strongly from M4 onto the polarizer tile, focusing >99.9% of the incident power within the polarizer pattern. The existing polarizer grating was designed for 28 GHz; hence, the midplane launchers operate at dual frequency, with 34.8 GHz being the primary for flat-top current drive. As we sized each mirror to capture $\geq$99% beam power at 28 GHz, more power is automatically captured at the primary frequency. Spillover power at full power operation, <1% at 34.8 GHz and $\sim$1% at 28 GHz, is a risk, so our stray power monitoring diagnostics will be carefully commissioned along with the gyrotrons to act as interlocks.

C. Off-Axis/Upper Launcher

The EBW upper launcher provides co-current injection only at approximately 600 mm above the MAST-U midplane.

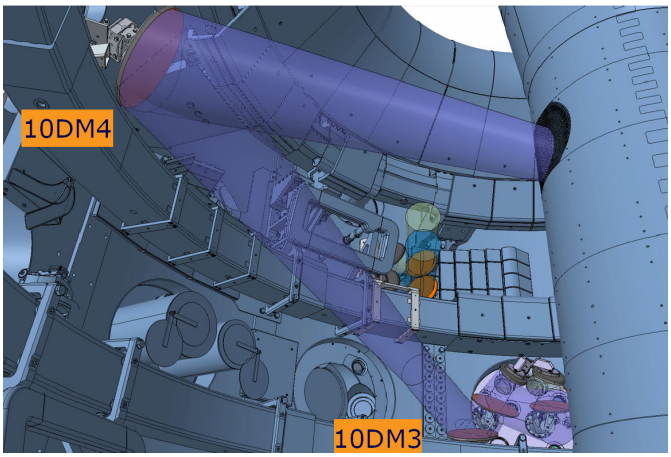

Fig. 3. Alternative configuration of the on-axis delta launcher for plasma start-up sends the beam, shown here by translucent blue cones, across the vessel to a grating polarizer tile on the CC. O-mode at 28 GHz is injected and converted on the high-field side into X-mode, which is absorbed at the electron cyclotron resonance. The delta steering mirror (DM2) is retracted close to the port, allowing the beam to pass through two focusing mirrors (DM3 and DM4) and onto the polarizer, with a total path length of 4.5 m.

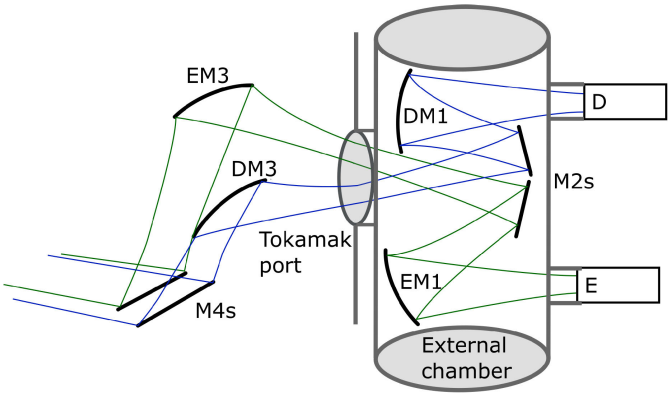

Fig. 4. Sketch of the off-axis launcher paths for the two gyrotron beams, delta and epsilon, showing the beam traveling right to left through the four mirror path between waveguide aperture and plasma. The first two mirrors in each path sit in an additional vacuum chamber mounted onto the tokamak vacuum vessel. Mirror pairs M1 and M3 are focusing, while pairs M2 and M4 are flat. The M4s are steerable to direct the beams over a range of toroidal and poloidal injection angles.

The two gyrotron beams enter the vacuum vessel in sector 9, adjacent to the midplane launchers in sector 10, through a DN250 port. We found no viable two-mirror optical layout for this launcher due to the spatial constraints of our 88.9-mm waveguide, beam expansion, and other in-vessel components. Consequently, we have designed a four-mirror configuration, similar to the TCV upper launcher [8], housing the first two mirrors in an additional vacuum chamber mounted onto the port. This facilitates key freedom in the waveguide routing process to minimize the number of miter bends, which are the predominant source of loss in the transmission line. Fig. 4 shows a cartoon of the launcher layout, beam profiles, and additional vacuum chamber, and Fig. 5 shows the in-progress CAD of the launcher in the MAST-U vessel environment. We had to have M1s with sufficient focusing power to fit the beams through the port as well as balance the separation of the M3s with the beam-port clearance. Due to the larger divergence of the 28-GHz beams, we were unable to route

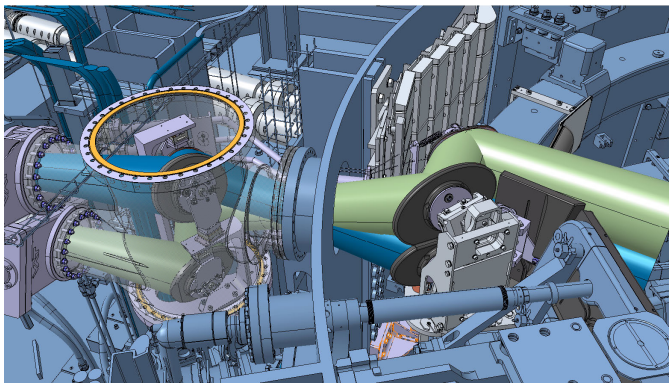

Fig. 5. Off-axis launcher assembly showing the delta (blue) and epsilon (green) beams entering the vacuum vessel from left to right. An ex-tokamak vacuum chamber (semitransparent) is mounted to the main vessel port, containing the first two mirrors to focus and direct the beams through the DN250 port. The third and fourth mirrors focus and steer the beams into the plasma.

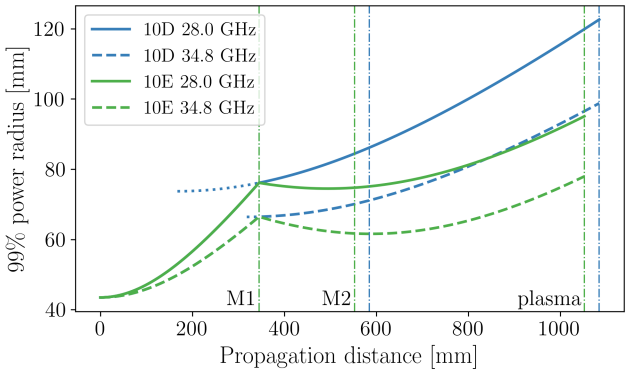

Fig. 6. Analytical beam envelopes (99% radii) for the midplane launchers at both 28 (solid) and 34.8 GHz (dashed) over the distance from waveguide aperture into the plasma. Mirror locations are shown by vertical dashed-dotted lines. The blue dotted lines show the beam profile from the virtual beam waists behind DM1 for both frequencies.

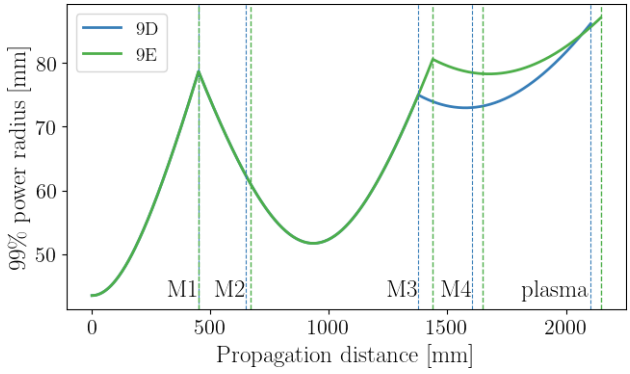

Fig. 7. Analytical beam envelopes (radii containing 99% of the beam power) for the upper launchers at 34.8 GHz over the distance from waveguide aperture into the plasma. The delta launcher is in blue, and epsilon is shown in green. Mirror locations are indicated by vertical lines.

them to the plasma, so the upper launcher will operate solely at 34.8 GHz. The translucent blue and green cones (delta and epsilon, respectively) in Fig. 5 show the beam paths through the four mirrors, which cross as they pass through the vacuum vessel port. The final beam sections into the plasma in this figure are shown as solid cones in Fig. 1, where the outer

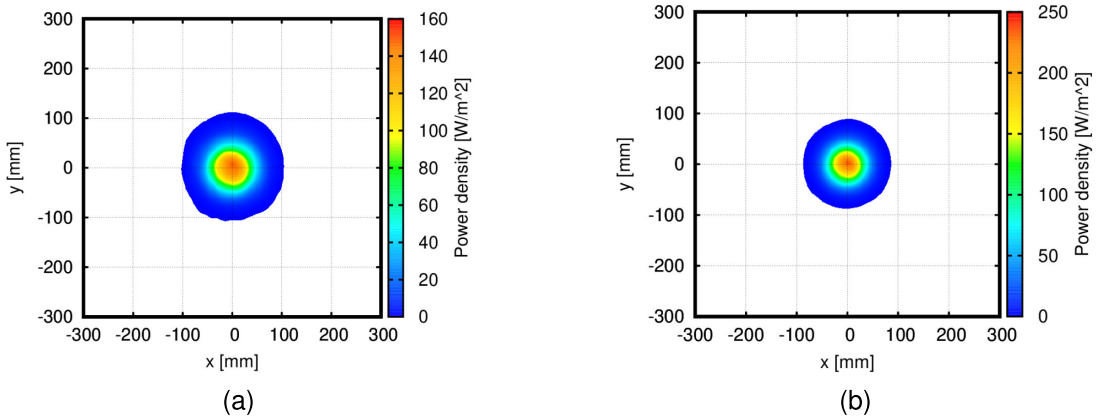

Fig. 8. Beam power density cross sections 200 mm after the midplane DM2 steering mirror at (a) 28 GHz and (b) 34.8 GHz for an input beam power of 1 W, modeled in PROFUSION [13]. The profiles are close to circular, and the outer contour shown contains 99% of the Gaussian beam power. The $3w$ beam diameter encompasses 99% of the beam power, where w, the Gaussian beam radius, is the radius of $1/e^2$ normalized intensity.

steering range encompassed by the semitransparent pink cones is required to access different plasma scenarios, with the same $\pm 5^\circ$ toroidal and poloidal steering about the optimum launch angles.

III. Beam Profiles and Modeling

Here, we include several figures of the midplane launcher envelope profiles, showing radii of the Gaussian beams throughout the launcher paths, simulated cross sections of the injected beams, and comparisons of the simulated beam radii with analytical Gaussian beam propagation [9], [10]. Fig. 6 shows the 99% power radius of the delta beam at both frequencies (blue lines) and the epsilon beam (green lines).

These radii are calculated for the designed frequency of 28 GHz using the analytical formula for Gaussian beam divergence; then, the propagation of the 34.8-GHz beams is found using quasi-optical propagation matrices [11], [12]. Increased divergence with decreased frequency can clearly be seen when comparing the two gyrotron frequencies (solid and dashed lines). Virtual propagation from the DM1 output beam waists, located behind the mirror surface, is included as dotted lines. In general, EBW coupling efficiency increases with increasing waist/wavelength ratio [4], so we have striven to keep the launcher output beam waists as large as possible. Our target waist/wavelength ratio was 6λ, and we have achieved the ratios between 4.5 and 5.1 for the midplane launcher. As the upper launcher will only operate at the higher gyrotron frequency, we have achieved the ratios of 5.6 and 6.0.

The beam profiles for the upper launcher are displayed in Fig. 7, showing the four-mirror configuration for the delta beam (blue) and the epsilon beam (green), with the mirror locations denoted by the corresponding vertical lines.

We cross-checked the analytical launcher optics with PROFUSION [13], modeling the quasi-optical beam propagation and calculating the cross polarization and higher order mode content of the injected beams. Cross sections of the delta beam power density after M2 are shown in Fig. 8, showing the difference in divergence between the two frequencies. As less truncation occurs at 34.8 GHz, the beam is less astigmatic than at 28 GHz, where the aperturing of $\sim$1% power at each mirror introduces sufficient higher order modes to the beam to be noticeable.

The astigmatism of both midplane beams can be seen in Fig. 9 by comparing the horizontal (subscript H) and vertical

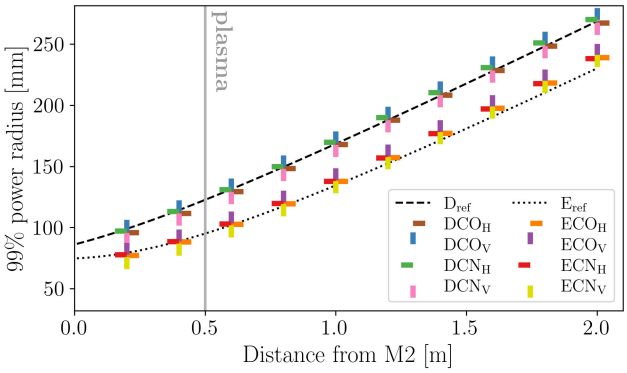

Fig. 9. Propagation after the midplane DM2 and EM2 steering mirrors: a comparison of analytical beam envelope against simulated beam propagation in PROFUSION at 28 GHz. The vertical axis values are the radii containing 99% of the beam power. Data are shown for orthogonal axes (**H**orizontal and **V**ertical subscripts) of the beams in the nominal co-current (CO) and counter-current (CN) steering directions. The vertical gray dotted line shows the average distance to the plasma (0.5 m) over the range of plasma scenarios.

(subscript V) beam radii as the beams propagate from the M2s. These radii for the nominal co- and counter-current injection directions are compared against the analytical optics beam radii (the radii containing 99% of the beam power), for both launchers at 28 GHz. The epsilon beam exhibits greater discrepancies from the ideal than delta, which is due to higher beam truncation, leading to a larger higher order mode content and cross-polarization fraction. Similarly, the analytical and modeled beam radii for 34.8 GHz are plotted in Fig. 10. Again, the propagation through both launchers shows acceptable agreement with the analytical design, with low astigmatism over the 2-m distance propagated past the steering mirrors, especially given the distance to the plasma is only 0.5 m. Some mirror steering positions lead to truncation of the beam within the 99% power contour, which will distort the injected beam and introduce more higher order modes. We are in the process of quantifying these additional losses.

IV. In-Vessel Protection and Diagnostics

In-vessel graphite tiles are required to protect components from uncoupled microwave power, which is reflected from the plasma. The semitransparent cones in Fig. 11 show the maximum possible extent of reflected beam coverage for all launch options. We are designing L-shaped tiles to sit over

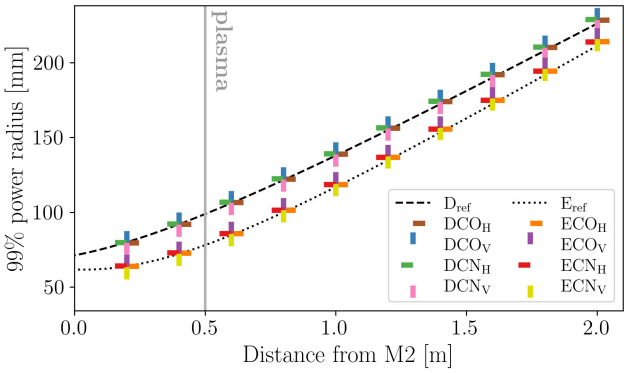

Fig. 10. Propagation after the midplane DM2 and EM2 steering mirrors: comparison of analytical beam envelope against simulated beam propagation in PROFUSION at 34.8 GHz. The vertical axis values are the radii containing 99% of the beam power. Data are shown for orthogonal axes (**H**orizontal and **V**ertical subscripts) of the beams in the nominal co-current (CO) and counter-current (CN) steering directions. The vertical gray dotted line shows the average distance to the plasma (0.5 m) over the range of plasma scenarios.

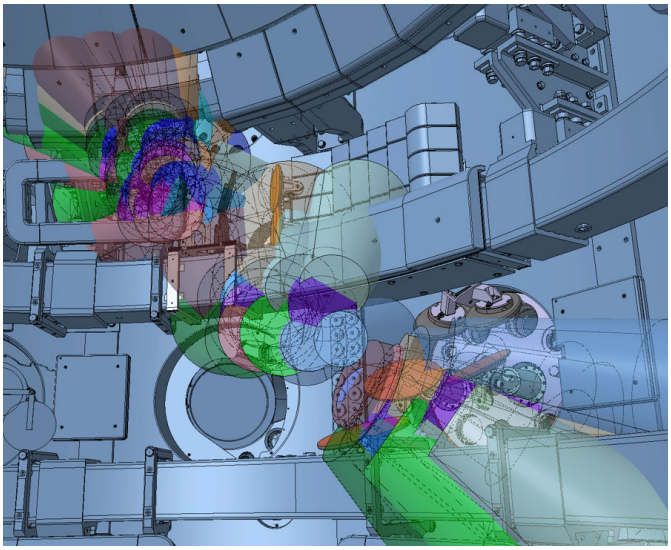

Fig. 11. Reflected beam cone models for the midplane and upper launchers showing the extremities of the possible area uncoupled, reflected power may land over the range of steering mirror injection angles.

the main poloidal coils on either side of the midplane (shown as semitransparent gray in Fig. 1), and a combination of tiles will cover the upper launcher reflected beam area. The tiles will have textured surfaces to scatter the incident radiation and lower the peak power density, as well as preferentially direct power away from sensitive components and vacuum windows. We will monitor their temperature profiles with IR cameras and through-hole thermocouples to infer the microwave-plasma coupling efficiency. These diagnostics will also act as a fast interlock on the gyrotrons if the graphite temperature sees too sharp a temperature rise, indicating poor coupling and high reflected power.

V. Conclusion

In this article, we have provided an update on the MAST-U EBW project optics and in-vessel component design requirements, engineering constraints, and current status, along with expected performance from modeling and comparison with the analytical design. We have achieved the EBW launcher system requirements within the engineering and MAST-U environment constraints. The outcome is a system with high flexibility to enable a thorough study of EBW current drive, start-up, and theoretical model validation with a view for impacting future tokamak HDC systems.

Acknowledgment

Members of the MAST-U EBW Team: Julian R Hawes, James Lovell, Grace Brett-Drinkwater, Asanka Munasinghe, Manminder Kalsey, Ewan Muir, and Elias Melidis. To obtain further information on the data and models underlying this article, please contact *publicationsManager@ukaea.uk*. The authors would like to thank MAST-U team for their support and contributions, Burkhard Plaum and Carsten Lechte at IGVP Stuttgart for their valuable modeling and design work, Tim Goodman at EPFL for his insight and guidance on all things microwave, the ECRH team at ASDEX-Upgrade for helpful discussions, and IDOM for their creative solutions to steer the EBW mirrors.

References

[1] F. R. Hansen, J. P. Lynov, and P. Michelsen, "The O-X-B mode conversion scheme for ECRH of a high-density tokamak plasma," *Plasma Phys. Controlled Fusion*, vol. 27, no. 10, p. 1077, Oct. 1985, doi: 10.1088/0741-3335/27/10/002.

[2] H. P. Laqua, V. Erckmann, H. J. Hartfuß, and H. Laqua, "Resonant and nonresonant electron cyclotron heating at densities above the plasma cutoff by O-X-B mode conversion at the W7-As stellarator," *Phys. Rev. Lett.*, vol. 78, pp. 3467–3470, May 1997, doi: 10.1103/PhysRevLett.78.3467.

[3] H. P. Laqua, "Electron Bernstein wave heating and diagnostic," *Plasma Phys. Controlled Fusion*, vol. 49, no. 4, p. R1, Mar. 2007, doi: 10.1088/0741-3335/49/4/R01.

[4] S. Freethy et al., "Microwave current drive for STEP and MAST upgrade," in *Proc. EPJ Web Conf.*, vol. 277, 2023, Art. no. 04001, doi: 10.1051/epjconf/202327704001.

[5] H. Webster et al., "MAST Upgrade microwave heating and current drive system–engineering design overview," in *Proc. EPJ Web Conf.*, vol. 277, 2023, Art. no. 04004, doi: 10.1051/epjconf/202327704004.

[6] H. Webster et al., *Design and Development of an Electron Bernstein Wave Heating and Current Drive System for MAST-U*, (IAEA FEC 2023 contribution number IAEA-CN-316/2386), 2023.

[7] V. Shevchenko et al., "Long pulse EBW start-up experiments in MAST," in *Proc. EPJ Web Conf.*, vol. 87, 2015, Art. no. 02007, doi: 10.1051/epjconf/20158702007.

[8] T. Goodman, S. Alberti, M. Henderson, A. Pochelon, and M. Tran, "Design and installation of the electron cyclotron wave system for the TCV tokamak," in *Fusion Technology*, C. Varandas and F. Serra, Eds. Oxford, U.K.: Elsevier, 1997, pp. 565–568. [Online]. Available: https://www.sciencedirect.com/science/article/pii/B9780444827623501117

[9] C. Gauss, *Dioptrische Untersuchungen*. Göttingen, Germany: Dieterischen Buchhandlung, 1841. [Online]. Available: https://books.google.co.uk/books?id=Tk2boAEACAAJ

[10] L. Empacher and W. Kasparek, "Analysis of a multiple-beam waveguide for free-space transmission of microwaves," *IEEE Trans. Antennas Propag.*, vol. 49, no. 3, pp. 483–493, Mar. 2001.

[11] A. Gerrard and J. Burch, *Introduction to Matrix Methods in Optics* (Dover Books on Physics). New York, NY, USA: Dover, 1994. [Online]. Available: https://books.google.co.uk/books?id=naUSNojPwOgC

[12] P. F. Goldsmith, *Gaussian Beam Propagation*. Hoboken, NJ, USA: Wiley, 1998, pp. 9–38.

[13] B. Plaum, "Simulation of microwave beams with PROFUSION," Universität Stuttgart, Stuttgart, Germany, Tech. Rep., 2022. [Online]. Available: http://elib.uni-stuttgart.de/handle/11682/12258